Wear 269 (2010) 416–423

Contents lists available at ScienceDirect

Wear

journal homepage: www.elsevier.com/locate/wear

The effect of laser polishing on fretting wear between a hemisphere and a flat plate

B. Raeymaekers*, F.E. Talke

University of California San Diego, 9500 Gilman Dr., La Jolla, CA 92093-0401, United States

ARTICLE INFO

Article history:
Received 25 August 2009
Received in revised form 23 April 2010
Accepted 28 April 2010
Available online 13 May 2010

Keywords:
Fretting
Wear
Laser polishing

ABSTRACT

Fretting wear between a hemisphere and a flat plate is investigated experimentally and the effect of laser polishing is studied. The energy dissipated between the hemisphere and the flat plate is determined as a function of operating conditions such as frequency and normal load and material properties such as surface roughness, and related to the wear observed at the sliding interface. Abrasive, adhesive and tribochemical wear are formed on the hemisphere and flat plate. No significant difference in wear production between a laser polished and a regular stainless steel hemisphere was observed.

1. Introduction

Fretting is defined as a cyclic relative motion between two surfaces in contact at small displacement amplitude [1–3]. Depending on material properties, loading conditions and environment, fretting can cause fretting fatigue or fretting wear [4,5]. Mechanisms for fretting wear are oxidation, adhesion, surface fatigue or abrasion [6]. Fretting wear occurs in many instances where mechanical parts are in sliding contact. Specific situations where fretting wear can occur are for example electrical switches where contacting conductors make a reciprocating contact when the switch is operated. Other examples include structural elements of bridges which undergo reciprocal sliding against each other due to dynamic loading (e.g., traffic, weather), and turbo machinery such as jet engine fans, compressors and turbines. Fretting wear can cause critical mechanical components to fail with potentially catastrophic consequences. Abrasive elements such as dust particles and sand (e.g., desert environment for jet engines) accelerate fretting wear. Atmospheric factors such as a corrosive environment also accelerate fretting wear [7]. For example, intertwined cables that span or are submerged in a corrosive medium and which slide over each other in a reciprocal fashion are damaged and eventually fail as a result of fretting. Fretting wear also occurs at the nanoscale. The slider containing the read/write element which flies over a magnetic disk in a hard disk drive rubs against a dimple on the suspension, thereby creating a reciprocal contact that may create wear particles and cause the hard disk drive to fail. MEMS and NEMS type devices are also subject to fretting wear. Lastly, sliding interfaces of prosthetic implants and artificial body parts are also subject to reciprocal motion, and, thus, subject to failure as a result of fretting wear.

At present, very little information is available in the open literature concerning how surface roughness affects fretting wear and how surface treatments influence the wear created between two bodies in reciprocating sliding contact. This paper tries to address this gap by studying the effect of laser polishing on wear at the interface between a hemisphere and a flat in reciprocating motion. Additionally, this paper tries to match the obtained experimental data with existing fretting and traditional uni-directional sliding models available in the literature.

2. Fretting research

Experimental investigations have shown that cyclic motion at the contact interface between two bodies can be divided into four different regimes of sliding: stick, partial slip, gross slip and reciprocal sliding [8,9]. A detailed description of the four fretting regimes is provided in [8]. The fretting regimes can be characterized as a function of normal load and displacement amplitude using so-called "fretting maps" [8]. The transition from "fretting" to "reciprocal sliding" is independent of the normal load but depends on the displacement amplitude [8,10].

Varenberg et al. [11] introduced a so-called "slip index", a criterion to determine different fretting regimes from a friction force versus relative displacement (friction hysteresis loop) measurement of the reciprocal motion between two samples [11,12]. The

* Corresponding author. Fax: +1 858 534 2720.
E-mail address: bart@talkelab.ucsd.edu (B. Raeymaekers).

0043-1648/$ – see front matter © 2010 Elsevier B.V. All rights reserved.
doi:10.1016/j.wear.2010.04.027

Nomenclature

A_d	displacement amplitude
A_s	sliding amplitude
C_v	ratio of maximum contact pressure under perfect slip condition at yield inception, and the yield strength
d_0	minimum separation between hemisphere and flat based on asperity heights
d_0^*	dimensionless minimum separation between hemisphere and flat based on asperity heights, d_0/σ
E	Young's modulus
H	hardness
h_0	minimum separation between hemisphere and flat based on surface heights
h^*	dimensionless minimum separation between hemisphere and flat based on surface heights h_0/σ
L_c	critical normal load under full stick condition
$\overline{L_c}$	ratio of the critical normal load under full stick condition and perfect slip, L_c/P_c
L_{eq}	equivalent sliding distance
n	number of fretting cycles
P	normal load
P^*	dimensionless normal load, P/L_c
P_c	critical normal load under slip condition
Q_{max}	maximum tangential load or friction force at sliding inception
Q^*_{max}	dimensionless maximum tangential load, Q_{max}/L_c
R	hemisphere radius of curvature
r	radial coordinate
r^*	dimensionless radial coordinate, $r/\sqrt{R\sigma}$
Y_0	yield strength
z	height of an asperity, based on the mean of asperity heights
z^*	dimensionless height of an asperity, z/σ
β	roughness parameter, $\rho\sigma_s\eta$
δ	slip index
δ_c	critical interference in stick
$\overline{\delta_c}$	ratio of the critical interferences in full stick and perfect slip, δ_c/ω_c
η	area density of asperities
μ	static friction coefficient
ν	Poisson coefficient
ρ	mean asperity tip radius of curvature
σ	standard deviation of asperity heights
σ_s	standard deviation of asperity summit heights
Φ^*	dimensionless distribution function of asperity heights
ψ	plasticity index
ω_c	critical interference in perfect slip

slip index δ is defined as

$$\delta = \frac{A_d S_c}{P} \quad (1)$$

where A_d is the displacement amplitude, A_s is the slip amplitude and S_c is the slope of the typical friction hysteresis loop, as illustrated in Fig. 1. P is the normal load.

The transition between the four sliding regimes for any given loading conditions can be specified by the slip index, which is universal for any scale from nano to macro fretting [12]. Varenberg identified the four regimes of sliding in terms of the slip index. Reciprocal sliding was found to occur when $\delta > 11$ and fretting was restricted to $\delta < 10$. Gross slip was found between $0.8 < \delta < 10$ and partial slip between $0.5 < \delta < 0.6$. The regime $\delta < 0.5$ was suggested to correspond to stick, pending more experimental validation.

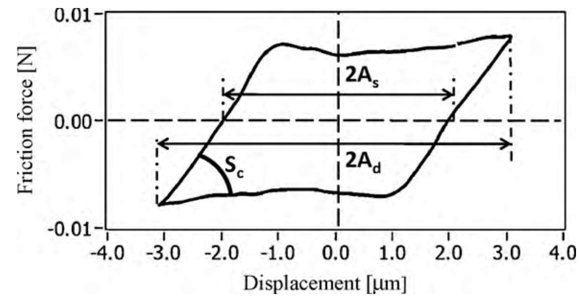

Fig. 1. Friction hysteresis loop definitions.

3. Experimental apparatus

Fig. 2(a) shows a schematic of the experimental apparatus used in this study. The set up consists of a shear mode piezo (PZT) actuator and a beam with a hemispherical shape punched into its surface, and is similar to several fretting testers documented in the literature [e.g., 13]. The beam is attached to a strain gauge-based load cell and positioned adjacent to the shear mode PZT. The hemisphere rests on the test specimen (flat plate), which is attached to a shear mode piezo (PZT) actuator, applying the tangential reciprocating loading. A normal force P is applied to the dimple by means of a dead weight. The shear mode PZT is actuated with a triangularly shaped input voltage signal with constant amplitude from a signal generator to create a reciprocating motion between the hemisphere and the test specimen. The displacement of the PZT actuator (see Fig. 2(c)) is measured with an optical displacement sensor. The load cell, attached to the stationary beam, measures the friction force F_t created between the hemisphere and the test specimen, as illustrated in Fig. 2(b). We have verified that the displacement of the suspension due to the friction force acting on the dimple is typically less than 10% of the displacement amplitude of the gimbal. Thus, the error committed in the measurement of the friction hysteresis loops using only one displacement measurement on the gimbal rather than two independent displacement measurements on the gimbal and the dimple, is small in the present study and can be neglected. It should be pointed out, however, that under high frictional load separate measurement of the displacement of both the dimple and the gimbal may be necessary to improve the accuracy of the friction hysteresis loops.

4. Test procedure and samples

We have used a regular stainless steel and laser polished stainless steel beam and hemisphere, and a stainless steel test specimen (flat plate). The laser polishing is a non-contact finishing technique where the surface topography is being smoothened by melting and vaporization of the top layer of the hemisphere material. Table 1 summarizes the surface and material properties for the hemisphere and test specimen we have used. The Young's modulus E was taken from the literature and hardness H was measured using a nanoindenter. The surface roughness properties were measured using an atomic force microscope. The measurements showed that the surface roughness of the dimple and gimbal is isotropic. Hence, the Greenwood–Williamson approach can be used to describe surface roughness of hemisphere and test specimen [14]. The average asperity tip radius ρ, the asperity density η, and the standard deviation of asperity summit heights σ_s can be obtained using the three spectral moments m_0, m_2, and m_4 of the surface roughness as described by McCool [15] (see appendix). The non-dimensional